amplitude varies linearily with deformation time as shown in Fig. 2a and b. However, this linear relationship was not observed at the low rates of phase-boundary sliding at large values of strain. The ratio between the maximum rate of phase-boundary sliding and the interlamellar spacing was found to be approximately constant for the two lamellar structures studied.

It should be noticed that the intracrystalline deformation accompanying the phase-boundary sliding may be considered negligible since this deformation is certainly less than the 2% error assumed in measuring the total tensile strain of 0.65 true strain. It was also observed that:

1. the sum of the amplitudes of the phase-boundary sliding of a few dozens of consecutive lamellae accounts approximately for the total tensile deformation of the specimen;

2. within each phase, the distance between the fiducial lines and as well as their orientation with respect to the phase-boundary plane remain always constant.

The degree of perfection of phase-boundary plane may greatly affect the mechanism of phase-boundary sliding. It may also explain on one hand the large dispersion of the sliding velocities of different lamellae. On the other hand, it may be also responsible for localized hardening which reduces the rate of phase-boundary sliding at large deformation.

It is planned to continue this investigation furthermore in order to establish correlation among different parameters such as shear stress, sliding velocity, interlamellar spacing and phase-boundary crystallography.

Acknowledgments

The authors thank the Centre National de la Recherche Scientifique for supporting this work financially. They also record their indebtedness to R. Racek for preparing the material.

References

1. M. G. BLANCHIN, A. GUINIER, C. PETIPAS and G. SAUVAGE, *Acta Met.* **20** (1972) 1251.
2. L. DOBROSAVLJEVIC, C. PETIPAS-DUPUIS and R. RACEK, *Phys. Stat. Sol.* **38** (1970) 159.
3. D. H. AVERY and W. A. BACKOFEN, *ASM Trans.* **58** (1965) 551.
4. Patent A.N.V.A.R. no. 73.34.618 (27.9.73).

Received 21 January
and accepted 6 February 1973

ANDRÉ EBERHARDT
BERNARD BAUDELET
Laboratoire de Physique et de Technologie de Matériaux, Université de Metz, France
Laboratoire associé au C.N.R.S. no. 155.

A scanning electron microscopic examination of sintered barium sodium niobate

In recent years, barium sodium niobate ($Ba_2NaNb_5O_{15}$ or BNN) has been proven to be an outstanding electro-optic material [1, 2]. So far, however, no study of the sintering mechanisms of polycrystalline BNN samples has been reported. In the present work some observations have been made regarding the sintering processes in BNN ceramic compacts using scanning electron microscopy (SEM). The use of SEM not only helps in observing the changes in grain and pore sizes with the degree of sintering, but it also enables the study of the associated morphological changes [3].

Reagent grade barium carbonate, sodium carbonate and niobium pentoxide were mixed in an agate mortar and pestle using methyl alcohol as a grinding medium. After drying, the powders were calcined at 1200 ± 5°C for 24 h. The resultant material was checked that it was single phase tungsten bronze barium sodium niobate ($Ba_2NaNb_5O_{15}$) from its X-ray diffraction pattern, using only Cu$K\alpha$ lines, taken with a Guinier camera. The calcined powder was then screened to −200 +300 mesh and compacts or pellets of about 0.5 in. diameter and 0.4 in. thick were made by pressing in a hydraulic press at a pressure about 15 000 psi* without the use of any binder.

The pellets were heated in a box furnace, maintaining temperature control within ± 5°C. The sintering temperatures chosen were 1200 and 1350°C, with sintering times up to 120 h in ambient atmosphere. After the furnace was raised to the appropriate temperature, the specimen was inserted in the furnace in a platinum crucible, heat-treated and then, after a specified sintering time, taken out of the maximum temperature zone to a lower

*10^3 psi = 6.89 Nmm^{-2}.

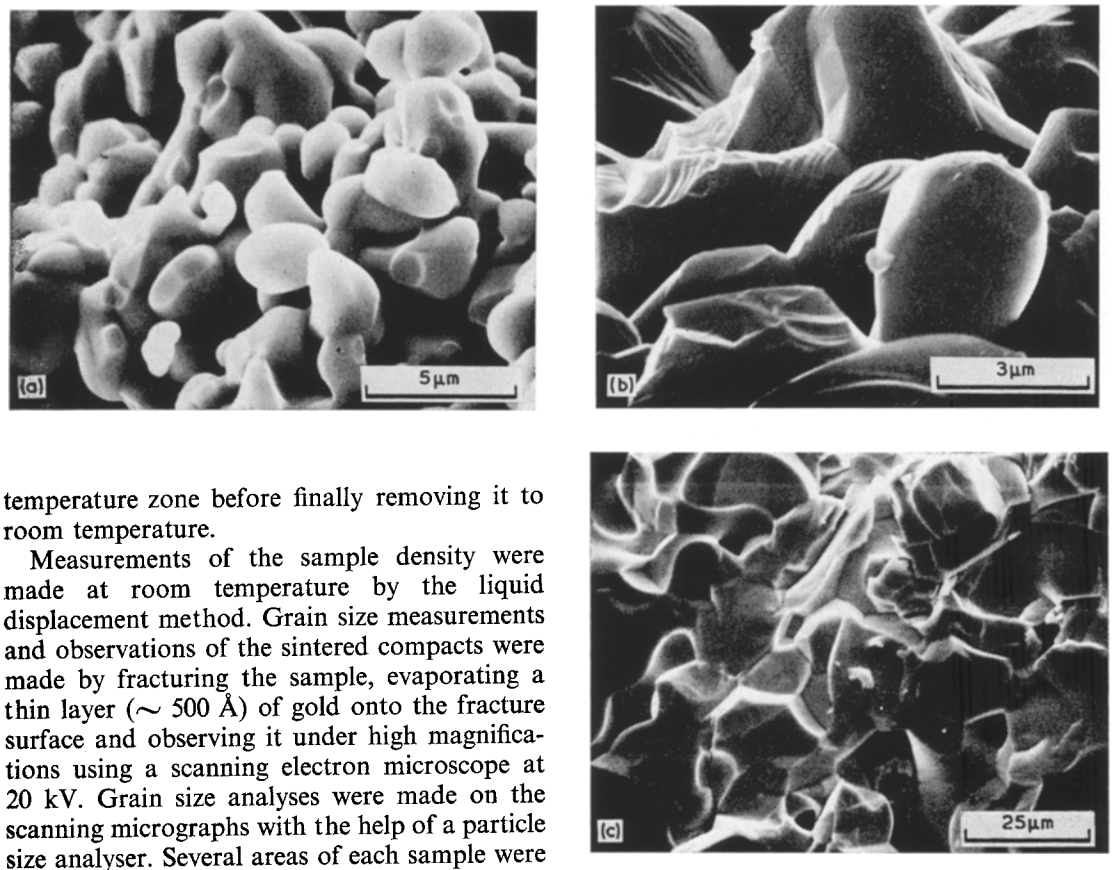

Figure 1 Scanning electron micrographs of BNN specimens sintered at: (a) 1200°C for 6.5 h, (b) 1200°C for 50 h, (c) 1350°C for 40 h.

temperature zone before finally removing it to room temperature.

Measurements of the sample density were made at room temperature by the liquid displacement method. Grain size measurements and observations of the sintered compacts were made by fracturing the sample, evaporating a thin layer ($\sim$ 500 Å) of gold onto the fracture surface and observing it under high magnifications using a scanning electron microscope at 20 kV. Grain size analyses were made on the scanning micrographs with the help of a particle size analyser. Several areas of each sample were studied in order to produce representative data.

It was evident from the experimental results that there was a net loss of material during the sintering process. As would have been expected, the rate of weight loss depended upon the particle size and hence the surface area exposed during the heat-treatment. The rate of weight loss in the sintered compacts was found to be about 0.002% min^{-1} at 1350°C and 0.0013% min^{-1} at 1200°C. The change in the pellet density (weight per unit total volume of the sintered pellet) was not appreciable at any stage of the sintering process. The density data, however, did show a decrease of approximately 3% in the apparent density (weight per unit volume of the water impermeable portion of the pellet) at 1350°C after $\sim$ 40 h, indicating a larger percentage of closed pores being formed. No noticeable change in apparent density was observed at 1200°C.

The grain size was obtained by measuring more than 200 grains in each sample and taking their root mean square diameter, D. Grain growth was much slower at 1200°C than at 1350°C. Along with the increase in the grain size, a sequence of grain morphological changes was also observed. The grains became smooth and rounded after short sintering times, apparently, to minimize their surface energy. Such a phenomenon was particularly noticeable for smaller grains ($D \sim 1$ to 3 μm), as shown in Fig. 1a. At considerably longer sintering times, as shown in Fig. 1b for a sample sintered at 1200°C for 50 h, growth steps and facets developed on the grain surfaces. The sintered structure shown in Fig. 1c for a sample held at 1350°C for 40 h, has a very large grain size ($D \simeq 20$ μm) compared to the starting grain size ($D = 2.25$ μm), and fewer but larger pores. Along with grain growth, the size of the pores also increased with sintering time and temperature. However, the density data indicated that no appreciable change in the total pore volume had occurred. This is supported by the observation of larger, but fewer, pores in the specimens sintered for long periods of time. Fig. 2a and b

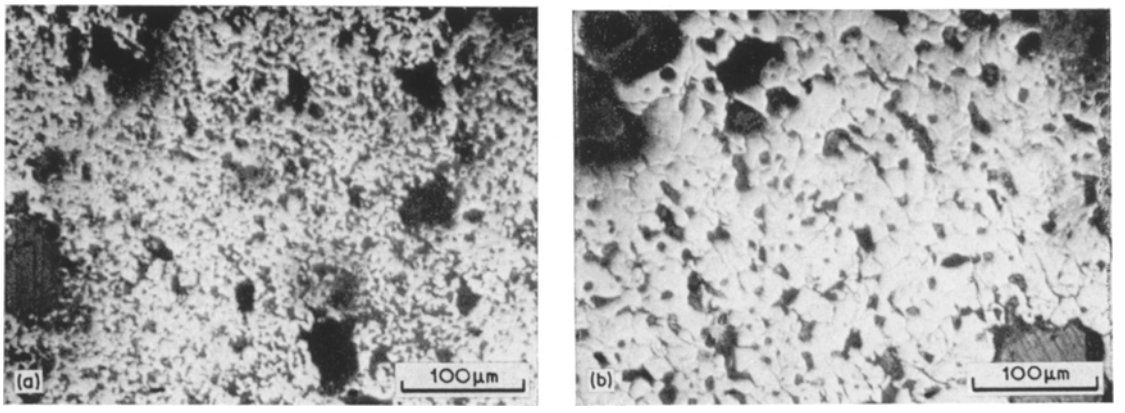

Figure 2 Reflected light photomicrograph of unetched specimens sintered at 1350°C: (a) for 30 min and (b) for 40 h. The sample in (b) has larger but fewer pores compared to that in (a).

show the distribution of pores in the specimens sintered at 1350°C for 30 min and 40 h, respectively.

From the observed morphological changes of the grains, it appears that more than one transport mechanism was operating simultaneously at the early stages of the sintering process. The oblong appearance due to neck-growth and the grain smoothing are mainly controlled by volume and surface diffusion, respectively [4]. At a later stage, especially for the samples sintered at 1350°C, a considerable amount of faceting occurred. The high vapour pressure of the constituents of BNN, reflected through the weight loss during the sintering process, as well as the observation of growth or evaporation surface steps, support vapour transport as having been the major sintering mechanism. These observations are consistent with Jackson's model for crystal growth by vapour transport [5]. Additional supporting evidence is that little or no change in the pellet density was found. This is generally the case in a vapour-controlled grain growth process [4]. Similar sintering behaviour has been postulated for polycrystalline Al_2O_3 and UO_2 materials [6-9]. A near cubic growth rate (i.e. $D^3 \simeq Kt$) was observed for the isothermal sintering at 1350°C as shown in Fig. 3. This grain growth relation has commonly been found in the sintering of oxides [10].

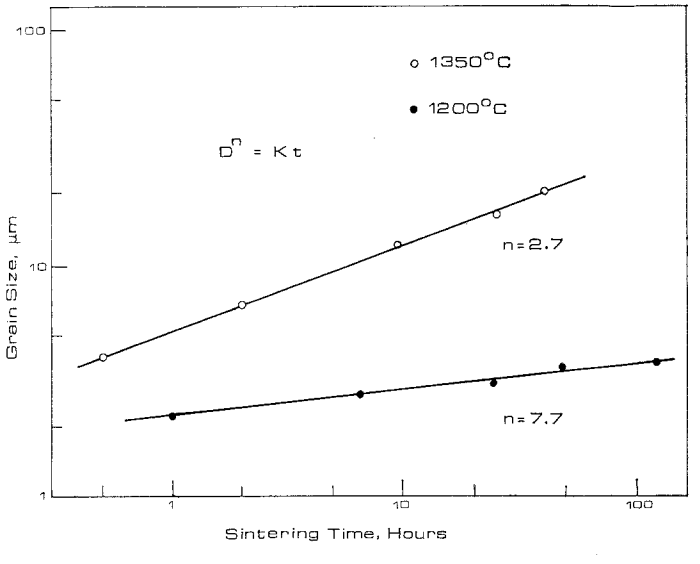

Figure 3 Grain size, D, versus sintering time, t, at 1200 and 1350°C. Slopes are equal to n^{-1} and K is a proportionality constant.

References

1. J. E. GEUSIC, H. J. LEVINSTEIN, S. SINGH, R. G. SMITH and L. G. VAN UITERT, *Appl. Phys. Letters* **12** (1968) 306.
2. R. G. SMITH, J. E. GEUSIC, H. J. LEVINSTEIN, J. J. RUBIN, S. SINGH and L. G. VAN UITERT, *ibid* **12** (1968) 308.
3. G. GRESKOVICH and K. W. LAY, *J. Amer. Ceram. Soc.* **55** (1972) 142.
4. F. A. NICHOLS, *J. Amer. Ceram. Soc.* **51** (1968) 468.
5. K. A. JACKSON, Interface Structure, in "Growth & Perfection of Crystals", (edited by R. H. Doremus) (Wiley, New York, 1958) p. 319.
6. N. A. L. MANSOUR and J. WHITE, *Powder Met.* **12** (1963) 108.
7. J. R. MACEWAN, *J. Amer. Ceram. Soc.* **45** (1966) 37.
8. R. L. COBLE, *J. Appl. Phys.* **32** (1961) 793.
9. F. A. NICHOLS, *ibid* **37** (1966) 4599.
10. R. S. GORDON, D. D. MERCHANT and G. W. HOLLENBERG, *J. Amer. Ceram. Soc.* **53** (1970) 399.

Received and accepted
19 February 1974

KEDAR P. GUPTA*
RICHARD W. SIEGEL
FRANKLIN F. Y. WANG
Department of Materials Science,
State University of New York,
Stony Brook, New York, USA

*Present address: Monsanto Electronic Materials, St. Peters, Missouri, USA.